This is the accepted manuscript version of the contribution published as:

The publisher's version is available at:

1 # Combining *Geobacter* spp. dominated biofilms and

2 # anaerobic digestion effluents - the effect of effluent

3 # composition and electrode potential on biofilm

4 # activity and stability

5 *Daniel Dzofou Ngoumelah[1,2], Anne Kuchenbuch[2], Falk Harnisch[2], Jörg Kretzschmar[1],**

6 [1]DBFZ Deutsches Biomasseforschungszentrum gemeinnützige GmbH (German Biomass

7 Research Centre), Department of Biochemical Conversion, 04347 Leipzig, Saxony, Germany

8 [2]Helmholtz Centre for Environmental Research - UFZ, Department of Environmental

9 Microbiology, 04318 Leipzig, Saxony, Germany

10 **KEYWORDS:**

11 Anaerobic digestion, applied anode potential, *Geobacter* spp. dominated biofilm, methanogens,

12 microbial electrochemical technologies.

13 **ABSTRACT**

14 The combination of anaerobic digestion (AD) and microbial electrochemical technologies (MET)

15 offers different opportunities to increase the efficiency and sustainability of AD processes.

16 However, methanogenic archaea and/or particles may partially hinder combining MET and AD

17 processes. Furthermore, it is unclear if the applied anode potential affects the activity and

18 efficiency of electroactive microorganisms in AD-MET combinations as it is described for more

19 controlled experimental conditions. In this study, we confirm that 6-week-old *Geobacter* spp.

20 dominated biofilms are by far more active and stable in AD-effluents than 3-week-old *Geobacter*

21 spp. dominated biofilms. Furthermore, we show that the biofilms are twice as active at -0.2 V

22 compared to 0.4 V, even under challenging conditions occurring in AD-MET systems. Paired-end

23 amplicon sequencing at the DNA level using 16S-rRNA and *mcrA* gene shows that

24 hydrogenotrophic methanogens incorporate into biofilms immersed in AD-effluent without any

25 negative effect on biofilm stability and electrochemical activity.

26 **SYNOPSIS**

27 Minimal research exists on how the microbial community composition of anaerobic digestion

28 (AD) effluents affects the performance of *Geobacter* spp. dominated biofilms. This study shows

29 that AD effluents containing different methanogens with different metabolic pathways have

30 different effects on the activity and stability of *Geobacter* spp. dominated biofilms.

31 **Graphical Abstract**

32

33

34

2
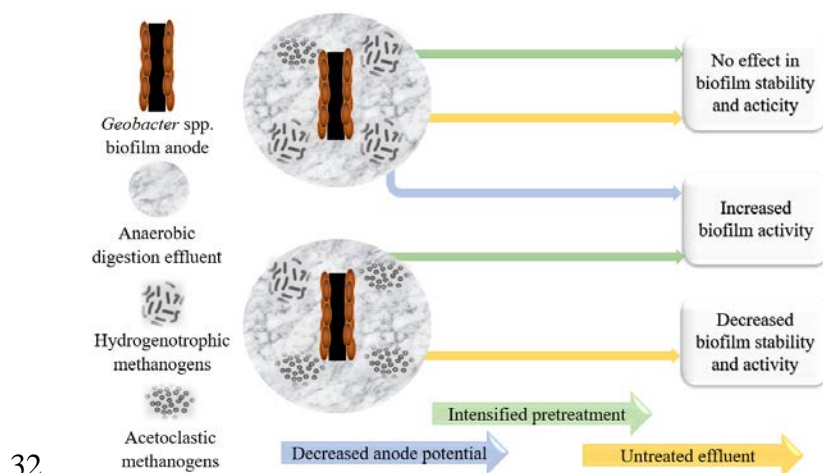
Introduction

Industrial wastewater or agricultural residues like livestock manure or slurry are widespread substrates for anaerobic digestion (AD) to produce biogas, a mixture of biomethane (CH_4) and carbon dioxide (CO_2)[1]. In AD complex organic substances (carbohydrates, proteins and lipids) are first broken down in a three step process (i.e. hydrolysis, acidogenesis, acetogenesis) into mainly acetate, CO_2 and H_2[2,3]. Finally, in methanogenesis, biomethane is produced by cleavage of acetate into CO_2 and CH_4, or by reduction of CO_2 with H_2 (see also equations S10-S14)[1,2]. In the case of agricultural residues, the remaining fraction (i.e. digestate) is still rich in nutrients, e.g. ammonium nitrogen, indigestible carbon sources such as lignin and trace elements making it a valuable fertilizer[4]. The produced biogas can be used in combined heat and power (CHP) units or upgraded to biomethane and injected into the gas grid[1].

In contrast to AD, microbial electrochemical technologies (MET) represent novel biotechnological applications that are not yet part of industrial processes[5]. Primary MET rely on electroactive microorganisms (EAM) acting as bioelectrocatalysts in anodic oxidation or cathodic reduction[6–8] (see also equation S3 and S4). They are based on microbial extracellular electron transfer (EET) that allows connecting the metabolic electron flux with electron flow at electrodes[5]. EET occurs either by means of c-type cytochromes and nanowires (direct EET) or by the use of mediators such as flavins or H_2 (mediated EET)[9–13]. Manifold technical variations of primary MET exist. Microbial fuel cells (MFC) can use chemical energy stored in organic substances, e.g. present in wastewater [14–18]. MFC have been shown to offer a sustainable alternative for wastewater treatment by reducing energy consumption and minimizing costs associated with aeration, secondary clarification and secondary sludge treatment, while recovering nutrients and energy[14,16–21]. Microbial electrolysis cells (MEC) can be used for production of value added products such as H_2

3

58   and CH_4[14,15,21,22] as well as desalination of brackish water or urine using special form of MEC, so

59   called microbial desalination cells (MDC)[18,23].

60   Finally, AD and MET can be combined in different ways to, e.g., 1) remove recalcitrant pollutants

61   from AD digestate[24], 2) upgrade biogas to biomethane[25,26], 3) recover NH_4^+[23,27], 4) reduce the

62   chemical oxygen demand (COD) in digestate[26,28], and 5) monitor volatile fatty acids (VFA) in real

63   time in anaerobic bioprocesses using microbial electrochemical sensors (MESe)[29].

64   However, inhibition of EAM like anodic *Geobacter* spp. biofilms has been reported under AD

65   conditions. In detail, it was shown that the activity and resistance of EAM is affected by 1)

66   substrate competition, e.g. due to methanogenesis[30,31], 2) occurrence of soluble electron acceptors,

67   e.g., humic substances, nitrate, sulphate[17,31], 3) toxic compounds, e.g. disinfectants[32], or 4) direct

68   interactions with parasitic microorganisms (e.g., protozoans[33]). Former studies also revealed that

69   competition between acetoclastic (*Methanosaeta* and *Methanosarcina*) and hydrogenotrophic

70   (*Methanobacteria*) methanogens and EAM seriously impairs MEC performance[34]. It was further

71   reported that *Methanosaeta* species can make direct electrical connection with *Geobacter* spp.

72   (e.g., *Geobacter metallireducens*) accepting electrons for the reduction of CO_2 to CH_4 via direct

73   interspecies electron transfer (DIET)[35,36] and therefore may also affect the activity of biofilm

74   anodes. To conclude, especially *Geobacter* spp. dominated biofilm anodes (for simplicity here

75   denominated as *Geobacter* spp. biofilms) have been reported to be vulnerable to external

76   disturbances that hinders the bioelectrocatalytic activity and prevent widespread application of

77   combination AD and MET[30]. To overcome these limitations and ensure long life-span of

78   *Geobacter* spp. biofilms in complex AD environments, the identification of the main causes of

79   inhibition as well as means to mitigate these are of paramount importance. Several pre-treatment

80   techniques such as inhibition of methanogenic archaea using 2-Bromoethanesulfonate (2-BES) or

81 microfiltration of AD-effluents have already been proven to stabilize the performance of

82 *Geobacter* spp. biofilms in AD-MET systems[37]. However, albeit using both can shed light on the

83 role of methanogens, pre-treatments using 2-BES is no technically viable option, e.g. for combined

84 AD-MET operating in continuous mode. Therefore, AD-MET combinations need more detailed

85 examination, e.g. using a wider source of AD-effluents such as digestate from AD of agricultural

86 and/or animal residues.

87 The effect of the applied anode potential on the activity of *Geobacter* strains has been already

88 investigated[38]. The anode potential is an important factor, e.g. it selects biofilms that are dominated

89 by particular species[38], and/or control the microbial synergistic interaction[39]. To the best of our

90 knowledge, there are no studies investigating the effect of the applied anode potential on the

91 bioelectrocatalytic activity, microbial community as well as functional stability of *Geobacter* spp.

92 biofilms immersed in highly complex media such as AD-effluents.

93 In this study, we first investigate how the activity of *Geobacter* spp. biofilms pre-grown for 3

94 weeks and 6 weeks is affected by subsequent immersion into AD-effluent based on cow manure

95 and wheat straw. Furthermore, we investigate whether and how particles of different sizes and

96 methanogenic archaea present in the AD-effluent affect the activity of 6-week-old *Geobacter* spp.

97 biofilms and how their activity changes by applying different anode potentials in AD-MET

98 systems. The results are furthermore supported by analyzing the bacterial and archaeal community

99 of *Geobacter* spp. biofilm anodes and planktonic phases.

100

101 **Material and Methods**

102 All reported potentials refer to the Ag/AgCl sat. KCl reference electrode (+ 0.197 V vs. SHE). All

103 chemicals were of analytical or biochemical grade. Experiments were performed as independent

104 biological replicates (n ≥ 3), under strictly anoxic conditions at a temperature of 38 °C. In total, 27

105 independent biological experiments were conducted, with 24 lasting 10 weeks each and 3 lasting

106 6 weeks each. The control always refers to the last week of biofilm growth before exposure to AD-

107 effluent.

108   - **Experimental setup**

109 The experimental setup (Figure S2) consisted of a three-electrode setup, integrated into 250 mL

110 three-neck round bottom flasks that were used as single-chamber MEC. The working and the

111 counter electrodes were made of graphite rods (anode: d = 10 mm, L = 20 mm, A = 7.1 cm^2,

112 cathode: d = 10 mm, L = 30 mm, A = 10.2 cm^2, quality CP-2200, CP-Graphitprodukte GmbH,

113 Germany). The current collectors were made of stainless steel (d=0.5 mm, Goodfellow GmbH,

114 Germany). The electrodes were fabricated and assembled in the MEC as previously described[37].

115 To measure the volumetric gas production during each batch cycle, hollow needles connected to

116 tygon®-tubes (E 3603, inner d: 1.6 mm, Saint - Gobain Performance Plastics, France) were

117 inserted in the stopper and the tubes were connected to BlueVCount volumetric gas counters

118 (BlueSens gas sensor GmbH, Germany) for continuous measurement of the produced gas volume.

119   - **Media, inoculum, biofilm formation**

120 *Geobacter* spp. biofilm inoculum was initially grown according to Gimkiewicz *et al.*[40] using

121 wastewater from a primary clarifier of a local wastewater treatment plant (AZV Parthe, 04551

122 Borsdorf, Germany). Biofilms were subsequently enriched using a simple electrochemical

123 enrichment procedure according to Liu *et al.*[41]. The used growth medium consisted of 50 mmol L$^-$

124 ^{1} phosphate buffer, amended with 10 mmol L^{-1} of sodium acetate, vitamins and trace elements[40,42].

125 For more details, please see SI.

126   - **AD-effluent**

127 AD-effluent was taken from three continuously stirred tank reactors (CSTR) with a volume of 10 L

128 fed with cow manure and wheat straw, operated at 39 °C. The AD-reactor setup (Figure S1),

129 composition of the used AD-effluent (Table S1), operating conditions as well as process

130 parameters are provided in the SI.

131 - **Experiments**

132 Before each experiment, AD-effluent (100 % v/v) was pretreated by sieving (standard sieve with

133 a pore-size of 1 mm), centrifugation (Sorvall RC 6+ centrifuge, Thermofisher Scientific, Germany)

134 or filtration with 12 µm Cellulose acetate filters (Sartorius Stedim Biotech GmbH, Germany).

135 Table 1 shows the different pre-treatments per experiment. The resulting pre-treated AD-effluent

136 was then supplemented with 12.5 mL L^{-1} vitamin solution, 12.5 mL L^{-1} trace element solution.

137 Before starting each experiment, the required amount of AD-effluent was collected from the AD-

138 reactors and its acetate concentration was measured by high performance liquid chromatography

139 (HPLC, model CBM-20A, Shimadzu, USA) as previously described[37]. The final acetate

140 concentration was adjusted to 10 mmol L^{-1} to assure sufficient supply with electron donor and

141 carbon source. The experiments were conducted by immersing 3-week-old and 6-week-old

142 *Geobacter* spp. biofilms in differently pretreated AD-effluent over four successive batch cycles,

143 denoted B1, B2, B3 and B4, with one batch cycle lasting always one week. Referring to previous

144 work[40,41] and our own biofilm pre-growth (data not shown), 3-week-old and 6-week-old *Geobacter*

145 spp. biofilms were considered to be in a steady state. Here steady state means that similar

146 maximum current densities were measured during batch cycles before exposure to AD effluent.

147 Growing *Geobacter* spp. biofilms using only acetate-based medium for the same duration of each

148 experimental condition (i.e., from inoculation to B4) as well as for longer periods is well known

149 to lead only to insignificant performance decrease, as shown by Baudler *et al.*[43].

Table 1. Parameters of performed experiments, ø: pore size, n: number of biological experiments

Name of the experiment	Age of biofilms / weeks (batches)	Pre-treatment of AD-effluent	Anode potential / V	n
Biofilm age	3	Sieving, ø1 mm	0.2	3
	6	Sieving, ø1 mm	0.2	3*
Methanogens and particles	6	Sieving, ø1 mm	0.2	3*
		Centrifugation, 5,000g, 5 min		4
		Centrifugation 10,000g, 10 min		3
		Filtration, ø 12 µm		3
Anode potential	6	Sieving, ø1 mm	-0.2	4
			0.0	4
			0.2	3*
			0.4	3

151 * indicates the same experiment

152 - **Process monitoring**

153 Batch experiments were monitored by measuring pH, conductivity of the media, total gas

154 production, gas composition, COD removal and ammonium nitrogen (NH_4^+-N). Detailed

155 information on measurements and statistical analysis using one-way analysis of variance

156 (ANOVA) with post-hoc Tukey test, are provided in the SI.

157 - **Electrochemical Measurements**

158 Microbial electrochemical activity of *Geobacter* spp. biofilms was measured by

159 chronoamperometry (CA) and cyclic voltammetry (CV) using a CA cycle for 23 h, followed by

160 three CV cycles with vertex potentials at -0.5 V and 0.3 V and a scan rate of 1 mV s^{-1}. CA data

161 were analyzed towards 1) maximum current density (j_{max} in mA cm^{-2})[44] and 2) total transferred

162 amount of charge (Q in C) [11,37]. Q was determined for each batch cycle using equation (1).

$$Q = \int_{t_0}^{t_f} i \, dt \tag{1}$$

163 Where t_0 and t_f are the start and end of each batch cycle, i is current (A), dt is the time interval

164 between two data collection points (3 min).

- **Microbial community analysis**

166 Samples for microbial community analysis were taken at the end of each experiment: i) from the

167 planktonic phase of each replicate and ii) from the biofilm anodes. In the latter case, biofilm

168 samples were scratched off from the electrodes using a sterile spatula. Both, 2 mL of planktonic

169 and the biofilm samples were centrifuged at 10,000g for 10 min (centrifuge 5430 R, Eppendorf

170 AG, Germany) and the pellets were stored in 2 mL microcentrifugation tubes at -20 °C. Genomic

171 DNA was extracted with the NucleoSpin Soil Kit (Macherey-Nagel, Germany) using the SL2

172 buffer and the enhancer solution. DNA concentration was measured with a Qubit® Fluorometer

173 3.0 (Life technologies, USA, Oregon, Eugene) using the high sensitivity Qubit® dsDNA HS Assay

174 Kit following the instructions in the manual**.**

175 Paired-end amplicon sequencing was performed to analyze the qualitative and quantitative

176 composition of the bacterial community in the biofilms as well as the liquid phase (planktonic

177 biomass). Therefore, the V3-V4 region of the bacterial 16S rRNA genes was amplified using the

178 primers 341f (5′-CCT ACG GGN GGC WGC AG-3′) and 785r (5′-GAC TAC HVG GGT ATC

179 TAA KCC-3′) as described by Klindworth *et al*[45]. For analyzing the methanogenic community,

180 mlas (5′-GGT GGT GTM GGD TTC ACM CAR TA-3′) and *mcrA*-rev (5′-CGT TCA TBG CGT

181 AGT TVG GRT AGT-3′) primers were used to amplify the archaeal *mrcA* gene (subunit A of

182 methyl coenzyme M reductase)[46]. The sequencing library was prepared according the Illumina 16S

183 Metagenomic Sequencing Library Preparation protocol[47]. PCR reactions were performed with the

184 MyTaq HS Red Mix (polymerase and dye), 2x (Bioline, Germany). The raw de-multiplexed fastq

185 files were processed with the QIIME 2 2019.4 pipeline[48] using the DADA2 workflow based on

186 the amplicon sequence variant (ASV) approach[49]. For bacterial 16S rRNA genes, the truncation

187 length for the forwards reads was 270 bp and 220 bp for the reverse reads, that results in a

188   minimum overlap of 46 bp. After chimera removal, 1250 features from the 1279 sequence counts

189   were used for further analysis. In total, 1229 ASVs could be obtained. For the *mcrA* genes, the

190   truncation length for the forwards reads was 285 bp and 240 bp for the reverse reads, that results

191   in a minimum overlap of 35 bp. After Chimera removal, 185 features from the 197 sequence counts

192   were used for further analysis. In total, 185 ASVs could be obtained. The maximum number of

193   expected errors allowed in a read was set with maxEE = 2 for both bacterial 16S rRNA genes and

194   *mcrA* genes. The taxonomic assignment of the bacterial 16S rRNA genes was done using the

195   SILVA 138 reference database[50]. For the *mcrA* gene, a modified taxonomic database excluding

196   uncultured methanogens was used[51]. Further statistical analyses and the removal of non-bacterial

197   sequences for 16S rRNA genes of bacteria as well as of non-archaeal sequences for *mcrA* were

198   performed with the R packages phyloseq[52], Ampvis 2 [53] and ggplot2 [54].

199   Demultiplexed raw sequence data were deposited at the EMBL European Nucleotide Archive

200   (ENA) under the study accession number PRJEB52932.

201   **Results and discussion**

202   -   **Effect of age on biofilm performance**

203   Figure 1 shows the average Q and j_{max} observed for 6-week-old and 3-week-old pre-grown

204   *Geobacter* spp. dominated biofilms, exposed to AD-effluent (100 % v/v) sieved at 1mm.

205   Q and j_{max} of 6-week-old biofilms in Figure 1a first increase from the control (i.e., last week of

206   biofilm growth before exposure to AD-effluent) to B1 by factor 1.3 ± 4.6 and 1.2 ± 1.1,

207   respectively. Compared to B1, the values of B4 remain nearly constant, which is indicated by a

208   very slight variation by factor 1.0 ± 0.4 and 1.0 ± 0.6 for Q and j_{max}, respectively. In contrast to 6-

209   week-old biofilms, Figure 1b shows that Q and j_{max} of 3-week-old biofilms initially show no

210   significant difference between the control and B1, which is indicated by overlapping confidence

211 interval (CI) and a very slight variation by factor 1.0 ± 0.2 and 1.0 ± 5.1 for Q and j_{max} respectively.

212 Compared to B1, the values of B4 drop by factor 1.3 ± 0.7 for both Q and j_{max} respectively.

213 Comparing B4 for both 6-week-old and 3-week-old biofilms, discrepancies by factors of 1.8 ± 2.1

214 and 1.5 ± 4.0 are observed for Q and j_{max} respectively.

215 Using ANOVA to compare the mean values of Q and j_{max} for 3-week-old and 6-week-old biofilms

216 from B1 to B4 showed p-values lower than α for Q and j_{max} respectively (Figure S4). This result

217 confirms outcomes of our previous study, that 6-week-old biofilm anodes are by far more active

218 and resistant towards AD-effluents[37]. In our previous study, 3-week-old biofilms also showed a

219 significant decrease in performance, starting already during the second batch cycle with AD-

220 effluent concentration of only 25 % v/v[37]. As this effect of AD effluent was found similar, but less

221 distinct, we hypothesize that the origin and therefore the chemical and biological composition of

222 specific AD-effluents have specific effects on the activity and stability of *Geobacter* spp.

223 dominated biofilms.

224 The higher activity of 6-week-old biofilms (Figure 1a) than 3-week-old biofilms (Figure 1b)

225 exposed to AD-effluents may be related to their increased thickness (i.e., increased number of

226 conductive layers)[11,37] and, concomitantly, to the increased abundance of extracellular polymeric

227 substances (EPS, consisting of, e.g., extracellular DNA, polysaccharides, proteins)[37,55]. One of the

228 main functions of the EPS matrix is to protect the bacterial community against predators (e.g.,

229 protozoa) and the penetration of toxic compounds into the biofilm[55,56]. Thus, it is more likely that

230 in 6-week-old biofilms, the high abundance of EPS matrix is shielding the bacterial community[33]

231 and hence, preventing biofilm dispersal into the bulk medium[37].

232 Besides protecting inner biofilm layers, another feature of the EPS matrix is being involved in the

233 interactions among microorganisms, facilitating syntrophic reactions for the conversion of VFA

234   by fermenting bacteria of the outer biofilm layers into smaller metabolites (acetate, H_2, formate)

235   being consumed by EAM[37,55,57] (see equation S5-S9). Therefore, we speculate that the assumed

236   low abundance of EPS matrix in 3-week-old biofilms also limits their ability to make use of

237   additional VFA provided by AD-effluents.
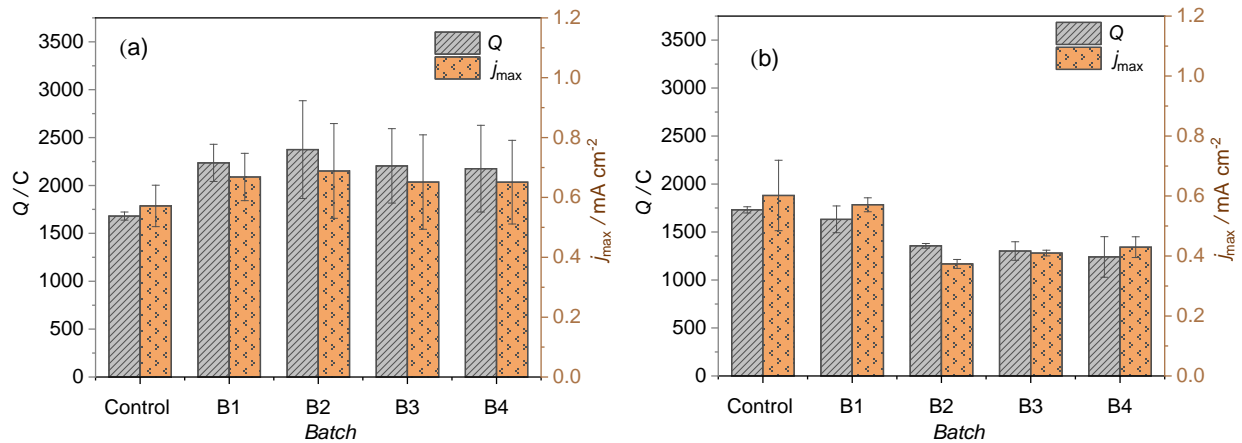
238   **Figure 1**. Transferred charge (Q) and current density (j_{max}) during experiments performed with:

239   (a) 6-week-old biofilms exposed to AD-effluents sieved at 1 mm, (b) 3-week-old biofilms exposed

240   to AD-effluents sieved at 1 mm. Control: phosphate buffer with acetate as sole carbon and energy

241   source, "B1 to B4" indicate the four successive batch cycles with AD-effluents, n = 3, error bars

242   indicate CI.

243   -   **How does the composition of AD-effluents affect the activity of *Geobacter* spp.**

244   **biofilms?**

245   For investigating the effect of methanogens and particles on the activity of *Geobacter* spp.

246   biofilms, 6-week-old biofilms were exposed to AD-effluents, pre-treated by sieving, centrifugation

247   at 5,000g and 10,000g as well as filtration at 12 µm (see also Table 1). Figure 2(a), 2(b), 2(c) and

248   2(d) show the average Q and j_{max} observed over four batches (i.e., from B1 to B4), for each pre-

249   treatment.

250 Comparing the control batches (AD-effluent 0 % v/v) always with the last batch (B4) of the

251 respective experiments shows a general increase of Q and j_{max}. Figure 2(a) shows that Q and j_{max}

252 with sieved AD-effluent first increase in B1 and then remain nearly stable until B4. In contrast,

253 centrifuged AD effluents (Figure 2(b) and 2(c)) show a gradual increase in the mean values of Q

254 and j_{max} from B1 to B4. Using filtered AD effluent (Figure 2(d)) shows nearly constant values of

255 Q from the control batch to B3, which then significantly increases in B4. In contrast, j_{max} in Figure

256 2(d) follows an inconsistent pattern from B1 to B3 and shows a similar value in B4 as in Figures

257 2(a), 2(b) and 2(c). Using ANOVA to compare the mean values of Q and j_{max} for 6-week-old

258 biofilms from B1 to B4, always gives p-values higher than α (Figure S5), meaning that at the

259 significance level of α = 0.05, the population means of Q and j_{max} are not significantly different

260 between pretreatments,

261 Barole *et al.* reported that increased Q and j_{max} over time in batch systems may be related to

262 operating conditions as mediator-producing organisms appear to be more prominent in batch

263 systems as they can accumulate in the bulk medium and remain even during periodic medium

264 replacement[58]. One may speculate that mediators began to accumulate already from B1, whose

265 number increases in successive batches, enabling electron transfer from EAM being unattached to

266 the anode[11]. Furthermore, *Geobacter* spp. are well known for their ability to use different VFA.

267 As reported by Engel *et al.*[11], although *Geobacter* spp. prefer acetate as main substrate, some

268 species also metabolize fermentation products, e.g., lactate or formate[8,9]. Table S1, reveals low

269 concentrations of VFA that might have been converted to acetate and H_2 by acetogenesis (also see

270 equation S5-S9) and therefore contributed to increased activity.

271 High ionic strength of the anolyte reduces the internal resistance (i.e., ohmic losses) and diffusion

272 limitations, that can result in increased biofilm performance[17,29,59]. Dhar *et al.* concluded that low

273　alkalinity (equation S16), e.g. in MET treating domestic wastewater decreases the current

274　density[28]. However, increasing ionic strength does not necessarily increase the performance of

275　EAM, as the salt tolerance of anodophilic bacteria varies widely[30,60–63]. Table S1 shows that the

276　conductivity of the used AD-effluent was 22.45 ± 0.78 mS cm^{-1}, which is ~2.8 fold higher than the

277　conductivity of the acetate-based medium used during biofilm growth. This high conductivity can

278　be directly linked to the high ionic strength of the AD-effluent (also see, Table S1), whereas

279　*Geobacter* spp. biofilms are reported to withstand such a comparably high ionic strength or

280　conductivity, respectively[30,63,64].

281　The activity of *Geobacter* spp. biofilm observed during the four batches may also have been

282　impaired by soluble electron acceptors in the media (e.g., sulfate or humic substances). As

283　mentioned elsewhere, during H_2 and acetate oxidation, sulfate and/or nitrate reduction can act as

284　electron sinks and thus reduce the bioelectroactivity (see equation S15)[19]. Table S1 shows that the

285　sulfate concentration of the AD-effluent was 11.68 ± 4.13 mg L^{-1}.

286　The volumetric gas production always increased during the four batches in comparison to the

287　respective control, but decreased within the single AD-effluents with intensified pretreatments

288　(Figure S7(c)). However, Figure S7(d) shows no significant difference of methane concentration

289　in the MEC headspace over time, albeit a comparison based solely on average values shows a

290　higher methane content using AD-effluent sieved at 1 mm compared to AD-effluent filtered at 12

291　µm. This may be due to a significant decrease in methanogens due to centrifugation or filtration,

292　however using these methods not elimination thereof can be achieved. Filtration using a smaller

293　pore size was not possible due to the very heterogeneous nature of the AD effluent, i.e. high

294　concentration of fibers and particles, as well as its high viscosity.

We assume that the proportion of non-EAM (e.g., acetogens or methanogens) or particles in the used AD-effluent (based on cow manure and wheat straw) does not limit the electroactivity of 6-week-old biofilms. However, pre-treatment can have effects when looking at the timescale, e.g. comparing B1 of AD-effluent sieved at 1mm with B1 of all other pre-treatments in Figure 2. Intensified pre-treatment slows down the establishment of a high biofilm performance. In early batches the number of microorganisms or conductive particles involved in the potential development of new metabolic networks is reduced.
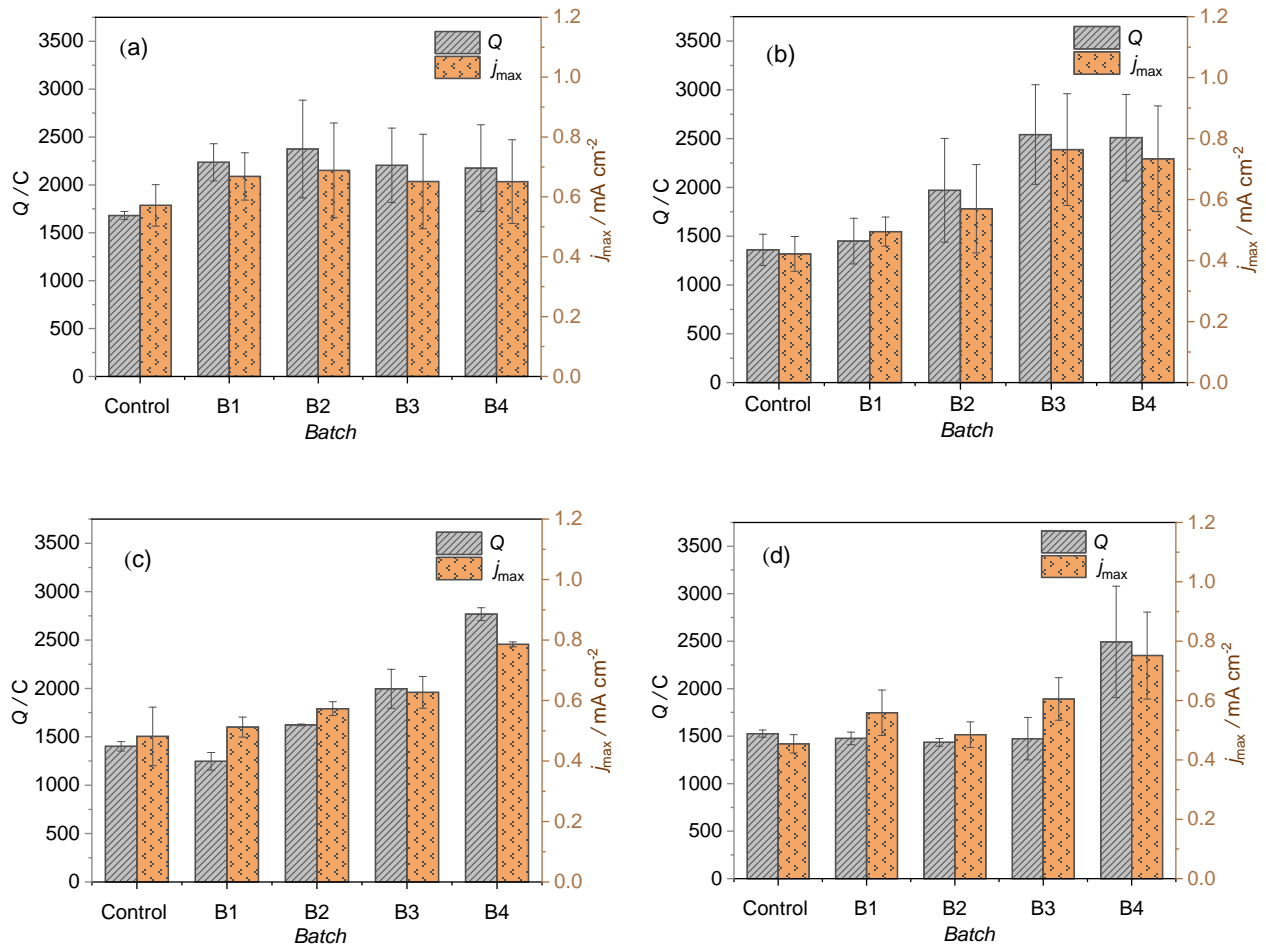
Figure 2. Q and j_{max} during experiments performed with 6-week-old biofilms exposed to: (a) AD-effluent sieved 1 mm, (b) AD-effluent centrifuged 5,000g, 5 min, (c) AD-effluent centrifuged

304   10,000g, 10 min, (d) AD-effluent filtered 12 µm. Control with acetate as sole carbon and energy

305   source, "B1 to B4" indicate the four successive batch cycles with AD-effluent, $n \geq 3$, error bars

306   indicate CI.

307   -   **Does the applied anode potential affect the activity of *Geobacter* spp. biofilms**

308   **immersed into AD-effluents?**

309   For investigating whether and to which extend the potential applied to the anode may affect the

310   activity (i.e., current output) of *Geobacter* spp. biofilms exposed to AD-effluents, several

311   experiments were conducted using 6-week-old biofilms at anode potentials of -0.2 V, 0.0 V, 0.2 V

312   and 0.4 V, respectively. After a growth period of 6 weeks, *Geobacter* spp. biofilms were

313   subsequently immersed in AD-effluents for 4 batches (B1 to B4) without changing the applied

314   anode potential. Figure 3(a) and 3(c) show that the mean values of Q and j_{max} first increase in B1

315   and then remain approximately stable until B4 for -0.2 V and 0 V. Figure 3(b) and 3(d) show a

316   slight decrease in Q and j_{max} from B1 to B4 for 0.2 V and 0.4 V. Overall, regardless the applied

317   anode potential, Q and j_{max} of 6-week-old *Geobacter* spp. biofilm do not change significantly

318   within each experiment over the four batches, as indicated by overlapping CI. Using ANOVA to

319   compare the means of Q and j_{max} for 6-week-old biofilms from B1 to B4 for all applied potentials,

320   shows p-values lower than α for the groups: [-0.2 V 0.2 V], [-0.2 V 0.4 V], [0.0 V 0.4 V] and [0.2

321   V 0.4 V], indicating a significant difference (see also Figure S6).

322   Comparing the control batches and B1 for each applied potential, shows a net increase in the mean

323   values of Q and j_{max} respectively. This may be related to either additional VFA input from the used

324   AD-effluent, hydrogen produced at the cathode or deriving from acetogenesis[37]. Hydrogen from

325   the cathode is used as substrate either by hydrogenotrophic/mixotrophic methanogens[22,65] or

326   *Geobacter* spp.[66,67]. Therefore, no or only minimal hydrogen was detected in the MEC headspaces

327   during control batches and upon exposure of *Geobacter* spp. biofilms to AD effluent for each

328   applied anode potential (see Table S3). We assume that a share of the hydrogen produced at the

329   cathode and/or deriving from acetogenesis was oxidized by the biofilm, hence contributed to an

330   increase in Q and j_{max}.

331   The controls in Figure 3(a) and 3(d), show that j_{max} is almost doubled at -0.2 V (e.g., 0.80 ± 0.08

332   mA cm^{-2}) compared to 0.4 V (e.g., 0.41 ± 0.04 mA cm^{-2}). A similar behaviour is also observed for

333   the two potentials from B1 to B4 (see also Table S2). It seems that in AD-effluent like in only

334   acetate-based media, *Geobacter* spp. biofilms are more active at lower applied anode potentials[68].

335   Therefore, we hypothesise that a lower ratio of VFA is degraded at 0.4 V compared to -0.2 V. This

336   is consistent with the observation made by Dennis *et al.* who showed that the rate of VFA

337   degradation declines with increasing applied anode potential[8]. *Geobacter* spp. biofilm electrodes

338   grown in acetate medium and poised at lower potentials are reported to have higher growth rate

339   and higher relative abundance of *Geobacter* spp. compared to higher potentials[15,38,68]. Torres *et al.*

340   also reported that *Geobacter* spp. biofilm electrodes poised at lower potentials show faster biofilm

341   growth, allowing more substrate oxidation, leading to higher current densities[68]. In contrast, the

342   positive potentials promote the development of non-EAM[68]. Here, we did not measure biofilm

343   growth, but referring to a previous work[68], we assume that *Geobacter* spp. biofilm anodes grown

344   at lower potentials (i.e. -0.2 V, 0.0 V, 0.2 V) have a higher cell density than biofilms grown at

345   higher potentials (i.e. 0.4 V). The electrocatalytic activity of *Geobacter* spp. biofilms has been

346   reported to be directly related to increasing cell density, which leads to an increase in the number

347   of cytochromes in the biofilm[37,69]. This means that biofilms grown at potentials ≤ 0.2 V probably

348   contain more cytochromes and nanowires, but also more EPS in contrast to biofilms grown at

349   potentials $\geq$ 0.4 V, as also discussed elsewhere[15,68]. EPS are known not only to protect the bacteria

350   from adverse environmental conditions but also to be one of the key agents involved in biofilm

351   formation, adhesion, structural development and in the process for the formation of

352   cytochromes[55,56]. Furthermore, Dennis *et al.* showed that high electrode potentials reduce current

353   production and constitute stressful conditions that degrade proteins and constrain bacterial

354   attachment to the electrode due to denaturation of outer membrane cytochromes[8]. This explains

355   further to the limited thermodynamic effect of the anode potential on the energy harvest[70] why

356   biofilm grown at more positive potentials (i.e. biofilm grown at 0.4 V) did not show higher Q and

357   j_{max}. Therefore, we strongly advocate follow up studies shedding light on the EPS quantity as well

358   as composition in different biofilm states, e.g. using chemical analysis of components, but also

359   optical coherence tomography or surface enhanced Raman resonance microscopy.

360   In contrast to the MEC using anode potentials of -0.2 V, 0.0 V and 0.2 V, only marginal volumes

361   of gas were recorded at 0.4 V from B1 to B4 (> 120 mL_{norm} w^{-1} vs. < 1.5 mL_{norm} w^{-1} at 0.4 V). The

362   controls also showed a larger volume of gas produced at -0.2 V, 0.0 V and 0.2 V than at 0.4 V (>

363   40 mL_{norm} w^{-1} vs. < 0.3 mL_{norm} w^{-1} at 0.4 V, see also Figure S7(e) and Table S3). Nevertheless,

364   headspace gas composition in terms of CH_4, CO_2 and H_2 remained quite similar for all applied

365   potentials (see Table S3 & Figure S7(f)). This indicates low activity of either planktonic

366   methanogens or those embedded in *Geobacter* spp. biofilms at 0.4 V, which is consistent with

367   previous works reporting that methanogens' activity decreases with more positive applied anode

368   potentials[15,22]. The low activity of methanogens at high potentials is most explicitly illustrated by

369   Fetzer and Conrad that used $K_3[Fe(CN)_6]$ and $K_4[Fe(CN)_6]$ to adjust the redox potential during

370   growth of *Methanosarcina barkeri* and observed no CH_4 production at potentials > 0.4 $V^{[71]}$ vs.

371   SHE. In Our case, 0.4 V vs. Ag/AgCl sat. KCl corresponds to 0.6 V vs. SHE.

To sum up, we show that *Geobacter* spp. biofilms are more active in AD-effluent at more negative anode potentials down to -0.2 V. However, the anode potential itself seems to have no significant effect on the stability of *Geobacter* spp. biofilms immersed in AD-effluents. Furthermore, it is more than likely that an anode potential ≥ 0.4 V impairs *Geobacter* spp. biofilm activity and promote conditions that slow down and/or are not permissive for methanogenesis.
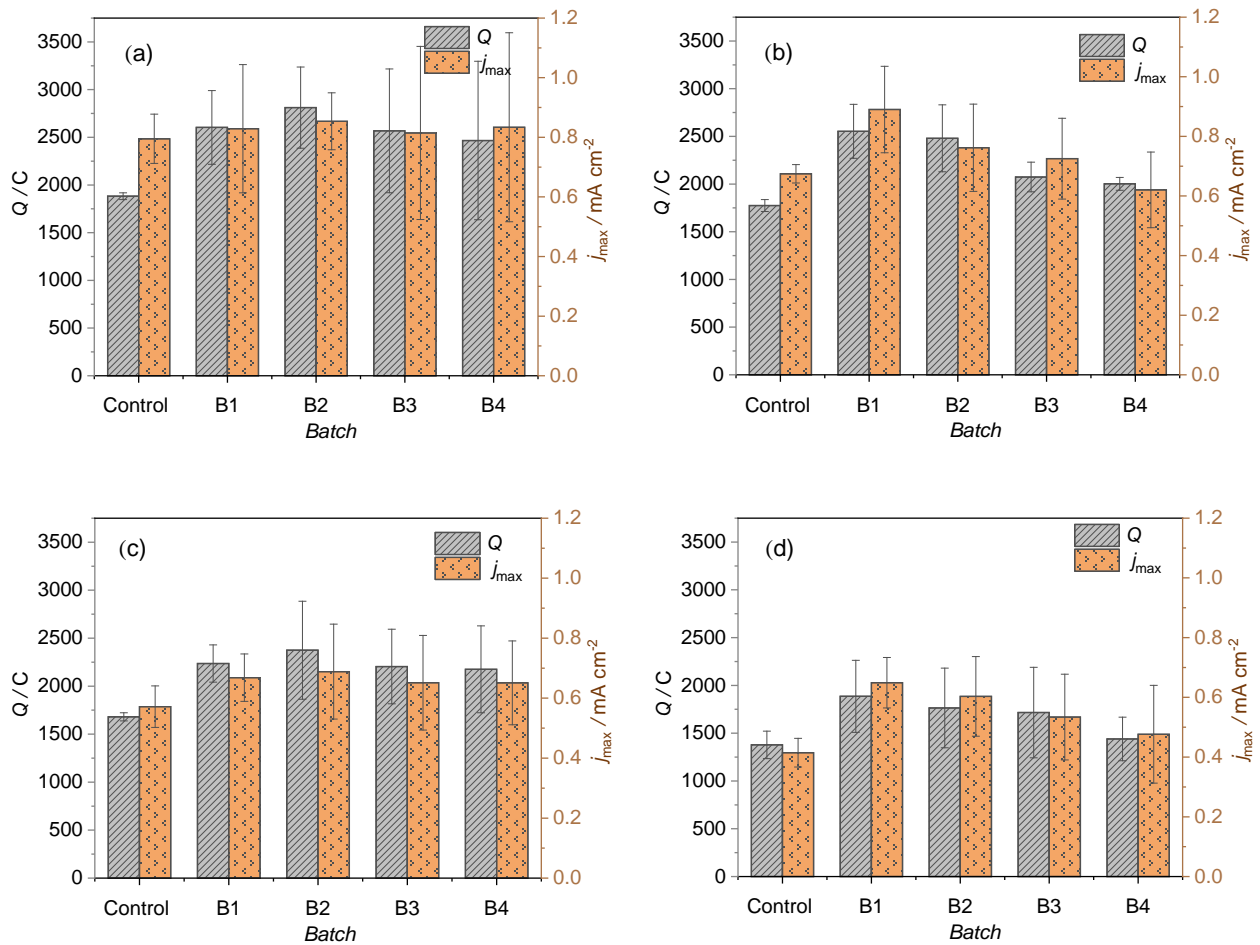
Figure 3. Q and j_{max} during experiments performed with 6-week-old biofilms exposed to AD-effluent sieved at 1mm at anode potentials of: (a) -0.2 V, (b) 0.0 V, (c) 0.2 V, (d) 0.4 V. Control with acetate as sole carbon and energy source, "B1 to B4" indicate the successive batch cycles with AD-effluent, $n \geq 3$, error bars indicate CI.

381   -   **Microbial community analysis**

382   The relationship between electrochemical biofilm performance (i.e., Q and j_{max}) and relative

383   abundance of *Geobacter* spp. in the biofilm anodes and planktonic phase as well as the

384   methanogenic community in the biofilms and planktonic phase was analyzed. Table 2 gives an

385   overview on the different samples analyzed using paired-end amplicon sequencing. Control

386   biofilms (i.e., biofilms grown solely in acetate-based medium) and pure AD-effluent were used for

387   comparison. Based on the electrochemical measurements, selected samples of biofilm anodes and

388   the planktonic phase were analyzed with emphasis on: 1) the relative abundance of *Geobacter* spp.

389   in biofilms and the planktonic phase, 2) the identification and quantification of methanogens in

390   biofilms and the planktonic phase, 3) the effect of sieving, filtration and applied anode potential

391   on the bacterial and methanogenic community in biofilms and planktonic phase, 4) the effect of

392   the composition of the methanogenic community in the AD-effluent on the microbial community

393   of *Geobacter* spp. biofilms.

394   **Table 2**. Overview on samples for microbial community analysis using paired-end amplicon

395   sequencing; + and - indicates whether the analysis has been performed or not.

Samples from	Samples from experiments with:	Anode potential / V	16S rRNA	*mcrA*	Annotation in Figure 4
Biofilm anodes	Control Biofilms (only acetate medium)	0.2	+	+	AW1
		0.4	-	+	AW2
	Biofilms + AD-effluent, filtration at 12 µm	0.2	+	+	AW3
	Biofilms + AD-effluent, sieved at 1mm	0.2	+	+	AW4
		0.4	-	+	AW5
Planktonic phase	Initial AD-effluent		-	+	BX1
	Biofilms + AD-effluent, filtration at 12 µm	0.2	+	+	BX2
	Biofilms + AD-effluent, sieved at 1mm	0.2	+	+	BX3
		0.4	-	+	BX4

396   The bacterial community composition in the different approaches is summarized in a heat map

397   (Figure 4a) showing the top 20 observed amplicon sequence variants (ASV) based on the bacterial

398   16S rRNA genes. *Geobacter* spp. is the most abundant ASV with ~77 % in the control biofilm

399   (AW1), which is consistent with our previous study, where we observed a relative abundance of

400   81.42 ± 13.55 %[37] for similar biofilms. The relative abundance of *Geobacter* spp. decreases to ~46

401   % in biofilms immersed in AD-effluent, filtered at 12 µm (AW3) and ~24 % in biofilms immersed

402   in AD-effluent, sieved at 1 mm (AW4). On the other hand, these decreases resulted in an increase

403   of the α-diversity (Shannon-indices) of the bacterial community composition, whereby the sieved

404   AD-effluent has a higher impact (Figure S9a).

405   In the corresponding planktonic phase BX2 and BX3 for AW3 and AW4, respectively, no

406   *Geobacter* spp. could be detected. Furthermore, the bacterial community in BX2 and BX3 show a

407   very high similarity (Figure S9b). Therefore, we postulate that decreasing the intensity of

408   pretreatment applied to the AD-effluent leads to a more diverse bacterial biofilm community

409   without negative effects on biofilm stability and electrochemical activity.

410   Figure 4b shows the heat map of the methanogenic community composition based on sequence

411   analysis of the *mcrA* gene of methanogenic archaea. Irrespective of the applied anode potential,

412   the methanogenic community in the control biofilm AW1 and AW2 is entirely dominated by the

413   genus *Methanobacterium*, which is consistent with the work of Korth *et al.*[67]. This indicates that

414   different applied anode potentials have no effect on the methanogenic community of *Geobacter*

415   spp. dominated biofilms. Here, sequencing of the methanogenic community, e.g. by using shotgun

416   sequencing could help to distinguish between the different *Methanobacterium* species. The

417   methanogenic community of the used AD-effluent (BX1) is entirely dominated by the families

418   *Methanobacteriaceae* and *Methanomicrobiaceae*, both known to consist of hydrogenotrophic

419   methanogenic species (i.e. using H_2/CO_2 and formate as carbon source)[72]. The methanogenic

420   community composition in biofilms immersed in AD-effluent sieved at 1mm (AW4 and AW5 in

421   Figure 4b) shows a higher α-diversity (Figure S10a) and is comparable to that in BX1 (also see

422 Figure S10b), with only minor variations in some less abundant genera such as

423 *Methanomassiliicoccus*. This indicates that during the four batches, *Methanomicrobiaceae* are

424 incorporated into the biofilm structure, without negatively affecting biofilm performance, as

425 shown for example in Figures 2 and 3. Figure 4b shows that the methanogenic community

426 composition of biofilms immersed in AD-effluent sieved at 12 µm (AW3) has a nearly similar

427 relative abundance of *Methanobacterium* spp. compared to control biofilms in AW1 and AW2.

428 This indicates that decreasing the pore size of the filters from 1 mm to 12 µm contributed to a

429 significant decrease in the proportion of *Methanomicrobiaceae* in the used AD-effluent, but did

430 not significantly affect the proportion of members of the *Methanobacterium* genus. The

431 methanogenic community composition of the planktonic phase after the four batches in BX2, BX3,

432 and BX4 is nearly similar to that of the respectively corresponding biofilm anodes AW3, AW4,

433 and AW5 (Figure S10b). Therefore, it appears that electrochemical cultivation of *Geobacter* spp.

434 biofilm in AD-effluents dominated by hydrogenotrophic methanogens results in incorporation of

435 the later into the biofilm with no negative effect on biofilm stability and electrochemical activity.

436 Our previous study revealed the inhibition of *Geobacter* spp. biofilm when combined with AD-

437 effluent from non-agricultural residues[37]. Therefore, it seems that the methanogenic community

438 composition of the used AD-effluent may impact the microbial composition and activity of

439 *Geobacter* spp. biofilm. To verify the latter hypothesis, we analyzed the methanogenic community

440 composition of the AD-effluent as well as the methanogenic and bacterial community composition

441 of *Geobacter* spp. biofilms immersed in AD-effluent used in our previous study[37] (see Table S4).

442 The control of the current study (AW1) showed a similar relative abundance of *Geobacter* spp. as

443 in our previous study and was therefore used as benchmark for the bacterial community

444 composition of *Geobacter* spp. biofilms after exposure to AD-effluent from our previous study.

445   AW6 in Figure S8a shows the bacterial community composition of *Geobacter* spp. biofilm after

446   exposure to AD-effluent (only two batches) from our previous study[37]. The relative abundance of

447   *Geobacter* spp. in AW6 is only ~3.3 % compared to the control (AW1) which shows a relative

448   abundance ~77 %. Furthermore, other genera such as *Proteiniphilum* or *Endomicrobium* that are

449   not present or rarely detected in AW1, became dominant in AW6. This shows significant changes

450   in the bacterial community of *Geobacter* spp. biofilm most likely induced by the microbiological

451   composition of the used AD-effluent. Figure S8b shows that the methanogenic community

452   composition of the used AD-effluent (BX5) in our previous study as well as that of *Geobacter* spp.

453   biofilms after the two batches (AW6) are mainly dominated by the genera *Methanobacterium* and

454   *Methanosaeta*. *Methanosaeta* spp. are indeed known as strict acetoclastic methanogens that can,

455   in combination with *Geobacter* spp., use DIET to reduce CO_2 to CH_4[35,72]. Therefore, we assume

456   that *Methanosaeta* members may play an important role in affecting the stability and

457   electrochemical activity of *Geobacter* spp. biofilms, as discussed elsewhere[35]. Our previous results

458   show that the methanogenic community composition of the AD-effluent varies with the used

459   substrate. Therefore, interactions between *Geobacter* spp. biofilms and specific methanogenic

460   archaea seems to be related to specific members of specific families of methanogens with

461   acetoclastic metabolism and/or the ability to perform DIET[73]. A systematic study using

462   combinations of *Geobacter* spp. biofilms with pure cultures of specific methanogens from different

463   families may help to gain more insight in the observed erratic patterns of *Geobacter* spp. biofilm

464   inhibition caused by AD-effluents.
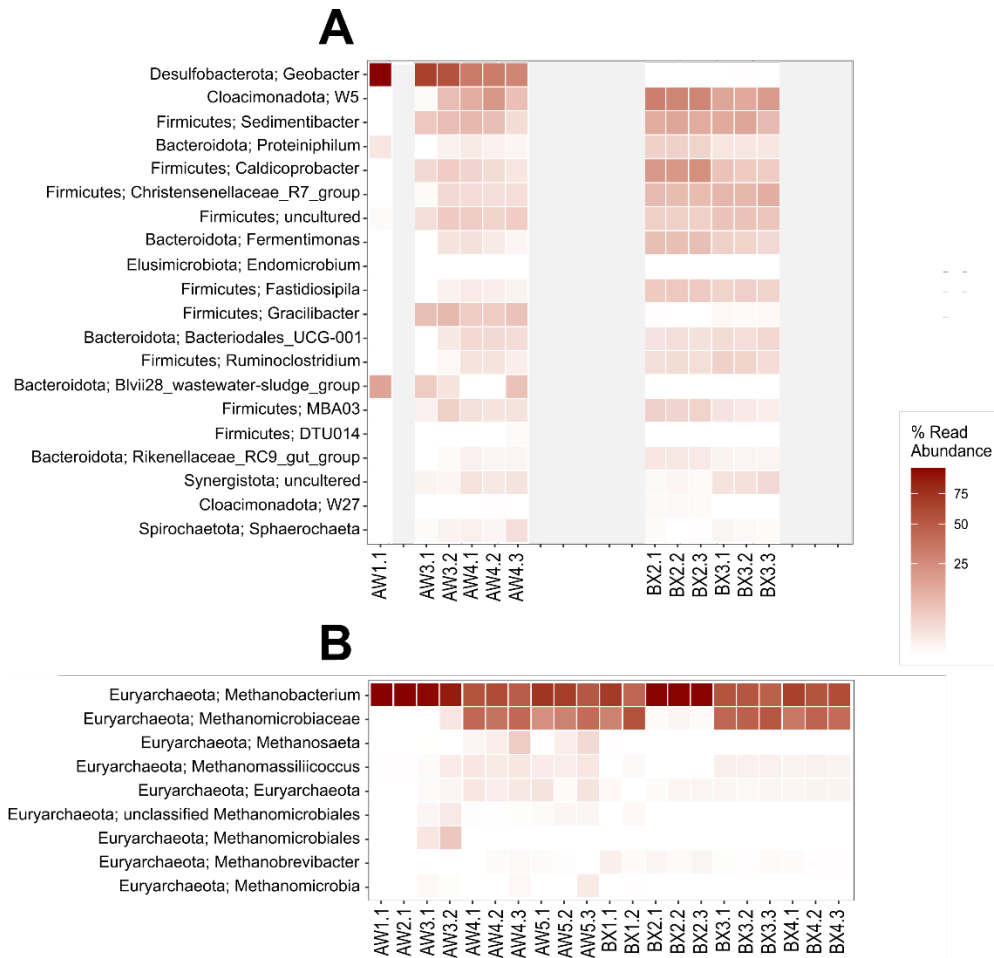
Figure 4. Microbial community composition (a) based on the 16S rRNA genes of bacteria showing the top twenty bacterial ASV and (b) based on the functional *mcrA* genes showing the top nine methanogenic ASV. For explanation of the abbreviations please see Table 2 and the text.

AUTHOR INFORMATION

Corresponding Author

*Jörg Kretzschmar

E-Mail: joerg.kretzschmar@dbfz.de

Author Contributions

The manuscript was written through contributions of all authors. All authors have given approval to the final version of the manuscript. The authors contributed as follows:

Conceptualization: DDN, JK, FH

Investigation: DDN

Molecular biology analysis: AK

Formal analysis: DDN, JK, FH

Funding Acquisition: DDN, JK, FH

Supervision: JK, FH

Visualization: DDN

Writing – Original Draft Preparation: DDN

Writing – Review & Editing: DDN, AK, JK, FH

ABBREVIATIONS

AD anaerobic digestion; ANOVA analysis of variance; ASV amplicon sequence variants; CA chronoamperometry; CI confidence interval; CHP combined heat and power; COD chemical oxygen demand; CV cyclic voltammetry; CSTR continuously stirred tank reactors; DIET direct interspecies electron transfer; EAM electroactive microorganisms; EET extracellular electron

496 transfer; ENA European Nucleotide Archive; EPS extracellular polymeric substances; HPLC high

497 performance liquid chromatography; j_{max} maximum current density; MEC microbial electrolysis

498 cell; MET microbial electrochemical technology; MESe microbial electrochemical sensors; MDC

499 microbial desalination cell; MFC microbial fuel cell; n number of replicates; Q transferred charge;

500 SI supplementary information; VFA volatile fatty acids.

Supporting Information

502 Additional information on materials and methods, description of experimental setup and operation

503 of AD reactors, volumetric gas production in the MEC, methane concentration in the headspace of

504 the MEC, equations of electrochemical and biological reactions at standard physiological

505 conditions, ANOVA results, Overview of the most important parameters at the end of different

506 batches, microbial community analysis.

References

508
509 (1) Fabien Monnet. An Introduction to Anaerobic Digestion of Organic Wastes. *Final Report*
510 **2003**, 1–48.
511 (2) Meegoda, J. N.; Li, B.; Patel, K.; Wang, L. B. A Review of the Processes, Parameters, and
512 Optimization of Anaerobic Digestion. *International journal of environmental research and public*
513 *health* **2018**, *15*, 1–16.
514 (3) Patel, V.; Pandit, S.; Chandrasekhar, K. *Microbial Applications: Basics of Methanogenesis in*
515 *Anaerobic Digester* 2; Springer, 2017.
516 (4) Enzmann, F.; Mayer, F.; Rother, M.; Holtmann, D. Methanogens: Biochemical background
517 and biotechnological applications. *AMB Express* **2018**, *8*, 1–22.
518 (5) Schröder, U.; Harnisch, F.; Angenent, L. T. Microbial electrochemistry and technology:
519 Terminology and classification. *Energy Environ. Sci.* **2015**, *8*, 513–519.
520 (6) Ruiz, Y.; Baeza, J. A.; Montpart, N.; Moral-Vico, J.; Baeza, M.; Guisasola, A. Repeatability
521 of low scan rate cyclic voltammetry in bioelectrochemical systems and effects on their
522 performance. *J Chem Technol Biotechnol* **2020**, *95*, 1533–1541.
523 (7) Molderez, T. R.; Prévoteau, A.; Ceyssens, F.; Verhelst, M.; Rabaey, K. A chip-based 128-
524 channel potentiostat for high-throughput studies of bioelectrochemical systems: Optimal electrode
525 potentials for anodic biofilms. *Biosensors & bioelectronics* **2021**, *174*, 112813.

526 (8) Dennis, P. G.; Virdis, B.; Vanwonterghem, I.; Hassan, A.; Hugenholtz, P.; Tyson, G. W.;
527 Rabaey, K. Anode potential influences the structure and function of anodic electrode and
528 electrolyte-associated microbiomes. *Scientific reports* **2016**, *6*, 39114.

529 (9) Speers, A. M.; Reguera, G. Electron donors supporting growth and electroactivity of
530 Geobacter sulfurreducens anode biofilms. *Applied and environmental microbiology* **2012**, *78*,
531 437–444.

532 (10) Korth, B.; Kretzschmar, J.; Bartz, M.; Kuchenbuch, A.; Harnisch, F. Determining
533 incremental coulombic efficiency and physiological parameters of early stage Geobacter spp.
534 enrichment biofilms. *PloS one* **2020**, *15*, 1-19.

535 (11) Engel, C.; Schattenberg, F.; Dohnt, K.; Schröder, U.; Müller, S.; Krull, R. Long-Term
536 Behavior of Defined Mixed Cultures of Geobacter sulfurreducens and Shewanella oneidensis in
537 Bioelectrochemical Systems. *Frontiers in bioengineering and biotechnology* **2019**, *7*, 1–12.

538 (12) Bond, D. R.; Lovley, D. R. Electricity production by Geobacter sulfurreducens attached to
539 electrodes. *Applied and environmental microbiology* **2003**, *69*, 1548–1555.

540 (13) Moscoviz, R.; Quéméner, E. D.-L.; Trably, E.; Bernet, N.; Hamelin, J. Novel Outlook in
541 Microbial Ecology: Nonmutualistic Interspecies Electron Transfer. *Trends in microbiology* **2020**,
542 *28*, 245–253.

543 (14) Koch, C.; Huber, K. J.; Bunk, B.; Overmann, J.; Harnisch, F. Trophic networks improve the
544 performance of microbial anodes treating wastewater. *NPJ biofilms and microbiomes* **2019**, *5*, 1–
545 9.

546 (15) Hasany, M.; Mardanpour, M. M.; Yaghmaei, S. Biocatalysts in microbial electrolysis cells:
547 A review. *International Journal of Hydrogen Energy* **2016**, *41*, 1477–1493.

548 (16) Jeuken, L. J. C.; Hards, K.; Nakatani, Y. Extracellular Electron Transfer: Respiratory or
549 Nutrient Homeostasis? *Journal of bacteriology* **2020**, *202*, 1–4.

550 (17) Ishii, S.'i.; Suzuki, S.; Norden-Krichmar, T. M.; Nealson, K. H.; Sekiguchi, Y.; Gorby, Y.
551 A.; Bretschger, O. Functionally stable and phylogenetically diverse microbial enrichments from
552 microbial fuel cells during wastewater treatment. *PloS one* **2012**, *7*, 1-12.

553 (18) Gajda, I.; You, J.; Mendis, B. A.; Greenman, J.; Ieropoulos, I. A. Electrosynthesis,
554 modulation, and self-driven electroseparation in microbial fuel cells. *iScience* **2021**, *24*, 102805.

555 (19) Georg, S.; Eguren Cordoba, I. de; Sleutels, T.; Kuntke, P.; Heijne, A. T.; Buisman, C. J. N.
556 Competition of electrogens with methanogens for hydrogen in bioanodes. *Water research* **2020**,
557 *170*, 115292.

558 (20) Escapa, A.; San-Martín, M. I.; Mateos, R.; Morán, A. Scaling-up of membraneless microbial
559 electrolysis cells (MECs) for domestic wastewater treatment: Bottlenecks and limitations.
560 *Bioresource technology* **2015**, *180*, 72–78.

561 (21) Geelhoed, J. S.; Stams, A. J. M. Electricity-assisted biological hydrogen production from
562 acetate by Geobacter sulfurreducens. *Environmental science & technology* **2011**, *45*, 815–820.

563 (22) Hu, H.; Fan, Y.; Liu, H. Hydrogen production using single-chamber membrane-free
564 microbial electrolysis cells. *Water research* **2008**, *42*, 4172–4178.

565 (23) Kuntke, P.; Sleutels, T. H. J. A.; Rodríguez Arredondo, M.; Georg, S.; Barbosa, S. G.; Ter
566 Heijne, A.; Hamelers, H. V. M.; Buisman, C. J. N. (Bio)electrochemical ammonia recovery:
567 Progress and perspectives. *Applied microbiology and biotechnology* **2018**, *102*, 3865–3878.

568 (24) Hua, T.; Li, S.; Li, F.; Zhou, Q.; Ondon, Brim, Stevy. Microbial electrolysis cell as an
569 emerging versatile technology: a review on its potential application, advance and challenge. *J*
570 *Chem Technol Biotechnol* **2019**, *94,* DOI: 10.1002/jctb.5898.

571 (25) Jin, X.; Zhang, Y.; Li, X.; Zhao, N.; Angelidaki, I. Microbial Electrolytic Capture, Separation
572 and Regeneration of CO2 for Biogas Upgrading. *Environmental science & technology* **2017**, *51*,
573 9371–9378.
574 (26) Vrieze, J. de; Arends, J. B. A.; Verbeeck, K.; Gildemyn, S.; Rabaey, K. Interfacing anaerobic
575 digestion with (bio)electrochemical systems: Potentials and challenges. *Water research* **2018**, *146*,
576 244–255.
577 (27) Desloover, J.; Woldeyohannis, A. A.; Verstraete, W.; Boon, N.; Rabaey, K. Electrochemical
578 resource recovery from digestate to prevent ammonia toxicity during anaerobic digestion.
579 *Environmental science & technology* **2012**, *46*, 12209–12216.
580 (28) Dhar, B. R.; Lee, H.-S. Evaluation of limiting factors for current density in microbial
581 electrochemical cells (MXCs) treating domestic wastewater. *Biotechnology reports* **2014**, *4*, 80–
582 85.
583 (29) Jin, X.; Li, X.; Zhao, N.; Angelidaki, I.; Zhang, Y. Bio-electrolytic sensor for rapid
584 monitoring of volatile fatty acids in anaerobic digestion process. *Water research* **2017**, *111*, 74–
585 80.
586 (30) Kretzschmar, J.; Böhme, P.; Liebetrau, J.; Mertig, M.; Harnisch, F. Microbial
587 Electrochemical Sensors for Anaerobic Digestion Process Control - Performance of Electroactive
588 Biofilms under Real Conditions. *Chem. Eng. Technol.* **2018**, *41*, 687–695.
589 (31) Barbosa, S. G.; Peixoto, L.; Ter Heijne, A.; Kuntke, P.; Alves, M. M.; Pereira, M. A.
590 Investigating bacterial community changes and organic substrate degradation in microbial fuel
591 cells operating on real human urine. *Environ. Sci.: Water Res. Technol.* **2017**, *3*, 897–904.
592 (32) Ogunwande, G. A.; Adeleye, A. I.; Nureni, I. O.; Omidiora, O. The effects of
593 cleaning/disinfecting agents on biogas production in the anaerobic digestion of cow dung slurry.
594 *Environmental technology* **2018**, *39*, 1803–1813.
595 (33) Holmes, D. E.; Nevin, K. P.; Snoeyenbos-West, O. L.; Woodard, T. L.; Strickland, J. N.;
596 Lovley, D. R. Protozoan grazing reduces the current output of microbial fuel cells. *Bioresource
597 technology* **2015**, *193*, 8–14.
598 (34) Yee, M. O.; Snoeyenbos-West, O. L.; Thamdrup, B.; Ottosen, L. D. M.; Rotaru, A.-E.
599 Extracellular Electron Uptake by Two Methanosarcina Species. *Front. Energy Res.* **2019**, *7*, 1.
600 (35) Rotaru, A.-E.; Shrestha, P. M.; Liu, F.; Shrestha, M.; Shrestha, D.; Embree, M.; Zengler, K.;
601 Wardman, C.; Nevin, K. P.; Lovley, D. R. A new model for electron flow during anaerobic
602 digestion: Direct interspecies electron transfer to Methanosaeta for the reduction of carbon dioxide
603 to methane. *Energy Environ. Sci.* **2014**, *7*, 408–415.
604 (36) Holmes, D. E.; Shrestha, P. M.; Walker, D. J. F.; Dang, Y.; Nevin, K. P.; Woodard, T. L.;
605 Lovley, D. R. Metatranscriptomic Evidence for Direct Interspecies Electron Transfer between
606 Geobacter and Methanothrix Species in Methanogenic Rice Paddy Soils. *Applied and
607 environmental microbiology* **2017**, *83*, 1–37.
608 (37) Dzofou Ngoumelah, D.; Harnisch, F.; Kretzschmar, J. Benefits of Age-Improved Resistance
609 of Mature Electroactive Biofilm Anodes in Anaerobic Digestion. *Environmental science &
610 technology* **2021**, *55*, 8258–8266.
611 (38) Commault, A. S.; Lear, G.; Packer, M. A.; Weld, R. J. Influence of anode potentials on
612 selection of Geobacter strains in microbial electrolysis cells. *Bioresource technology* **2013**, *139*,
613 226–234.
614 (39) Aelterman, P.; Freguia, S.; Keller, J.; Verstraete, W.; Rabaey, K. The anode potential
615 regulates bacterial activity in microbial fuel cells. *Applied microbiology and biotechnology* **2008**,
616 *78*, 409–418.

617   (40) Gimkiewicz, C.; Harnisch, F. Waste water derived electroactive microbial biofilms: Growth,
618   maintenance, and basic characterization. *Journal of visualized experiments: JoVE* **2013**, 1–15.
619   (41) Liu, Y.; Harnisch, F.; Fricke, K.; Sietmann, R.; Schröder, U. Improvement of the anodic
620   bioelectrocatalytic activity of mixed culture biofilms by a simple consecutive electrochemical
621   selection procedure. *Biosensors & bioelectronics* **2008**, *24*, 1012–1017.
622   (42) Kim, J. R.; Min, B.; Logan, B. E. Evaluation of procedures to acclimate a microbial fuel cell
623   for electricity production. *Applied microbiology and biotechnology* **2005**, *68*, 23–30.
624   (43) Baudler, A.; Riedl, S.; Schröder, U. Long-Term Performance of Primary and Secondary
625   Electroactive Biofilms Using Layered Corrugated Carbon Electrodes. *Front. Energy Res.* **2014**, *2*,
626   260.
627   (44) Ledezma, P.; Kuntke, P.; Buisman, C. J. N.; Keller, J.; Freguia, S. Source-separated urine
628   opens golden opportunities for microbial electrochemical technologies. *Trends in biotechnology*
629   **2015**, *33*, 214–220.
630   (45) Klindworth, A.; Pruesse, E.; Schweer, T.; Peplies, J.; Quast, C.; Horn, M.; Glöckner, F. O.
631   Evaluation of general 16S ribosomal RNA gene PCR primers for classical and next-generation
632   sequencing-based diversity studies. *Nucleic Acids Res.* **2013**, *41*, 1-11.
633   (46) Steinberg, L. M.; Regan, J. M. Phylogenetic comparison of the methanogenic communities
634   from an acidic, oligotrophic fen and an anaerobic digester treating municipal wastewater sludge.
635   *Applied and environmental microbiology* **2008**, *74*, 6663–6671.
636   (47) Illumina. 16S Metagenomic Sequencing Library Preparation: Preparing 16S Ribosomal RNA
637   Gene Amplicons for the Illumina MiSeq System. *Part # 15044223 Rev. B* **2013**.
638   (48) Bolyen, E.; Rideout, J. R.; Dillon, M. R.; Bokulich, N. A.; Abnet, C. C.; Al-Ghalith, G. A.;
639   Alexander, H.; Alm, E. J.; Arumugam, M.; Asnicar, F.; Bai, Y.; Bisanz, J. E.; Bittinger, K.;
640   Brejnrod, A.; Brislawn, C. J.; Brown, C. T.; Callahan, B. J.; Caraballo-Rodríguez, A. M.; Chase,
641   J.; Cope, E. K.; Da Silva, R.; Diener, C.; Dorrestein, P. C.; Douglas, G. M.; Durall, D. M.; Duvallet,
642   C.; Edwardson, C. F.; Ernst, M.; Estaki, M.; Fouquier, J.; Gauglitz, J. M.; Gibbons, S. M.; Gibson,
643   D. L.; Gonzalez, A.; Gorlick, K.; Guo, J.; Hillmann, B.; Holmes, S.; Holste, H.; Huttenhower, C.;
644   Huttley, G. A.; Janssen, S.; Jarmusch, A. K.; Jiang, L.; Kaehler, B. D.; Kang, K. B.; Keefe, C. R.;
645   Keim, P.; Kelley, S. T.; Knights, D.; Koester, I.; Kosciolek, T.; Kreps, J.; Langille, M. G. I.; Lee,
646   J.; Ley, R.; Liu, Y.; Loftfield, E.; Lozupone, C.; Maher, M.; Marotz, C.; Martin, B. D.; McDonald,
647   D.; McIver, L. J.; Melnik, A. V.; Metcalf, J. L.; Morgan, S. C.; Morton, J. T.; Naimey, A. T.;
648   Navas-Molina, J. A.; Nothias, L. F.; Orchanian, S. B.; Pearson, T.; Peoples, S. L.; Petras, D.;
649   Preuss, M. L.; Pruesse, E.; Rasmussen, L. B.; Rivers, A.; Robeson, M. S.; Rosenthal, P.; Segata,
650   N.; Shaffer, M.; Shiffer, A.; Sinha, R.; Song, S. J.; Spear, J. R.; Swafford, A. D.; Thompson, L.
651   R.; Torres, P. J.; Trinh, P.; Tripathi, A.; Turnbaugh, P. J.; Ul-Hasan, S.; van der Hooft, J. J. J.;
652   Vargas, F.; Vázquez-Baeza, Y.; Vogtmann, E.; Hippel, M.; Walters, W.; Wan, Y.; Wang, M.;
653   Warren, J.; Weber, K. C.; Williamson, C. H. D.; Willis, A. D.; Xu, Z. Z.; Zaneveld, J. R.; Zhang,
654   Y.; Zhu, Q.; Knight, R.; Caporaso, J. G. Reproducible, interactive, scalable and extensible
655   microbiome data science using QIIME 2. *Nature biotechnology* **2019**, *37*, 852–857.
656   (49) Callahan, B. J.; McMurdie, P. J.; Rosen, M. J.; Han, A. W.; Johnson, A. J. A.; Holmes, S. P.
657   DADA2: High-resolution sample inference from Illumina amplicon data. *Nature methods* **2016**,
658   *13*, 581–583.
659   (50) Yilmaz, P.; Parfrey, L. W.; Yarza, P.; Gerken, J.; Pruesse, E.; Quast, C.; Schweer, T.; Peplies,
660   J.; Ludwig, W.; Glöckner, F. O. The SILVA and "All-species Living Tree Project (LTP)"
661   taxonomic frameworks. *Nucleic acids research* **2014**, *42*, D643-8.

(51) Yang, S.; Liebner, S.; Alawi, M.; Ebenhöh, O.; Wagner, D. Taxonomic database and cut-off value for processing mcrA gene 454 pyrosequencing data by MOTHUR. *Journal of microbiological methods* **2014**, *103*, 3–5.

(52) McMurdie, P. J.; Holmes, S. phyloseq: An R package for reproducible interactive analysis and graphics of microbiome census data. *PloS one* **2013**, *8*, e61217.

(53) Kasper Skytte Andersen. ampvis2: an R package to analyse and visualise 16S rRNA amplicon data **2018,** DOI: 10.1101/299537.

(54) Wickham, H. *ggplot2, Use R!: Elegant graphics for data analysis*, 2nd ed.; Springer: Houston, Texas, USA, 2016.

(55) Li, T.; Zhou, Q.; Zhou, L.; Yan, Y.; Liao, C.; Wan, L.; An, J.; Li, N.; Wang, X. Acetate limitation selects Geobacter from mixed inoculum and reduces polysaccharide in electroactive biofilm. *Water research* **2020**, *177*, 1–7.

(56) Hou, R.; Luo, C.; Zhou, S.; Wang, Y.; Yuan, Y.; Zhou, S. Anode potential-dependent protection of electroactive biofilms against metal ion shock via regulating extracellular polymeric substances. *Water research* **2020**, *178*, 1–9.

(57) Costa, O. Y. A.; Raaijmakers, J. M.; Kuramae, E. E. Microbial Extracellular Polymeric Substances: Ecological Function and Impact on Soil Aggregation. *Frontiers in microbiology* **2018**, *9*, 1636.

(58) Borole, A. P.; Hamilton, C. Y.; Vishnivetskaya, T. A.; Leak, D.; Andras, C.; Morrell-Falvey, J.; Keller, M.; Davison, B. Integrating engineering design improvements with exoelectrogen enrichment process to increase power output from microbial fuel cells. *Journal of Power Sources* **2009**, *191*, 520–527.

(59) Guo, H.; Kim, Y. Stacked multi-electrode design of microbial electrolysis cells for rapid and low-sludge treatment of municipal wastewater. *Biotechnology for biofuels* **2019**, *12*, 23.

(60) Li, X. M.; Cheng, K. Y.; Wong, J. W. C. Bioelectricity production from food waste leachate using microbial fuel cells: Effect of NaCl and pH. *Bioresource technology* **2013**, *149*, 452–458.

(61) Sun, D.; Wang, A.; Cheng, S.; Yates, M.; Logan, B. E. Geobacter anodireducens sp. nov., an exoelectrogenic microbe in bioelectrochemical systems. *Int. J. Syst. Evol* **2014**, *64*, 3485–3491.

(62) Liu, G.; Yu, S.; Luo, H.; Zhang, R.; Fu, S.; Luo, X. Effects of salinity anions on the anode performance in bioelectrochemical systems. *Desalination* **2014**, *351*, 77–81.

(63) Lefebvre, O.; Tan, Z.; Kharkwal, S.; Ng, H. Y. Effect of increasing anodic NaCl concentration on microbial fuel cell performance. *Bioresour. Technol.* **2012**, *112*, 336–340.

(64) Sun, D.; Call, D.; Wang, A.; Cheng, S.; Logan, B. E. Geobacter sp. SD-1 with enhanced electrochemical activity in high-salt concentration solutions. *Environmental microbiology reports* **2014**, *6*, 723–729.

(65) Martínez, E.; Sotres, A.; Arenas, C.; Blanco, D.; Martínez, O.; Gómez, X. Improving Anaerobic Digestion of Sewage Sludge by Hydrogen Addition: Analysis of Microbial Populations and Process Performance. *Energies* **2019**, *12*, 1228.

(66) Kadier, A.; Simayi, Y.; Abdeshahian, P.; Azman, N. F.; Chandrasekhar, K.; Kalil, M. S. A comprehensive review of microbial electrolysis cells (MEC) reactor designs and configurations for sustainable hydrogen gas production. *Alexandria Engineering Journal* **2016**, *55*, 427–443.

(67) Korth, B.; Kuchenbuch, A.; Harnisch, F. Availability of hydrogen shapes the microbial abundance in biofilm anodes based on Geobacter enrichment. *ChemElectroChem* **2020,** DOI: 10.1002/celc.202000731.

(68) Torres, C. I.; Krajmalnik-Brown, R.; Parameswaran, P.; Marcus, A. K.; Wanger, G.; Gorby, Y. A.; Rittmann, B. E. Selecting anode-respiring bacteria based on anode potential: Phylogenetic,

708 electrochemical, and microscopic characterization. *Environmental science & technology* **2009**, *43*,
709 9519–9524.

710 (69) Fricke, K.; Harnisch, F.; Schröder, U. On the use of cyclic voltammetry for the study of
711 anodic electron transfer in microbial fuel cells. *Energy Environ. Sci.* **2008**, *1*, 144–147.

712 (70) Korth, B.; Harnisch, F. Spotlight on the Energy Harvest of Electroactive Microorganisms:
713 The Impact of the Applied Anode Potential. *Frontiers in microbiology* **2019**, *10*, 1352.

714 (71) Fetzer, S.; Conrad, R. Effect of redox potential on methanogenesis by Methanosarcina barkeri
715 **1993**, *160*, 108–113.

716 (72) Demirel, B.; Scherer, P. The roles of acetotrophic and hydrogenotrophic methanogens during
717 anaerobic conversion of biomass to methane: A review. *Rev Environ Sci Biotechnol* **2008**, *7*, 173–
718 190.

719 (73) Rotaru, A.-E.; Yee, M. O.; Musat, F. Microbes trading electricity in consortia of
720 environmental and biotechnological significance. *Current opinion in biotechnology* **2021**, *67*,
721 119–129.

722